第29卷第5期
2005年5月

高能物理与核物理
HIGH ENERGY PHYSICS AND NUCLEAR PHYSICS

Vol.29, No.5
May, 2005

Particle (Pseudo) Rapidity Distribution and the Overlapping Cylinder Model in Nucleus-Nucleus Collisions at High Energies *

SONG Fu LIU Fu-Hu1)
(Institute of Modern Physics, Shanxi Normal University, Linfen 041004, China)

Abstract The overlapping cylinder model (OCM) is used in this letter to describe the rapidity (or pseudorapidity) distributions of charged particles produced in nucleus-nucleus collisions at high energies. For the fixed target experiments at the present accelerator energies, the same relative strengths of longitudinal flows are observed and two completely overlapping cylinders can give a description of the experimental data. A stronger longitudinal flow is observed and two partly overlapping cylinders are needed at higher energies (above 4A TeV). The (pseudo)rapidity distributions calculated by the overlapping cylinder model are in agreement with the available experimental data.

Key words nucleus-nucleus collisions, (pseudo)rapidity distributions, overlapping cylinder model

The study of heavy ion interactions at high energy is an important field of particle and nuclear physics. On the one hand, the quark-gluon plasma (quark matter) predicted by various theories has been studied in high energy heavy ion interactions. On the other hand, some properties obtained of nuclear reactions have been explained by the knowledge of current physics.

The rapidity (or pseudorapidity) distribution of charged particles can be obtained in experiments. It is convenient for us to study the production process of particles by the (pseudo)rapidity distribution. Based on the one-dimensional string model[1] and the fireball model[2], we have developed a thermalized cylinder model[3—5] and described the (pseudo)rapidity distributions of relativistic singly charged particles in nucleus-nucleus collisions at high energies. Recently, the thermalized cylinder model has been developed to the overlapping cylinder model[6].

As a continuous work, in this letter, we use the overlapping cylinder model[6] which takes into account the transverse flow, longitudinal flow and the temperature of emission source to describe the (pseudo)rapidity distributions of charged particles produced in nucleus-nucleus collisions in an energy range from 1A GeV to 100A TeV. As far as we know, no previous successful attempt has been made fit the data of heavy ion interactions in such a wide energy range with one model. This is the subject of this letter.

In high-energy nucleus-nucleus collisions, it is expected that the projectile and the target make a cylinderical cut through each other along the direction of the incident projectile and form participants. The rest of the two nuclei remain relatively undisturbed forming spectators. The participant target lies in the rapidity range $[y_{T_{\min}}, y_{T_{\max}}]$, and its midrapidity is y_{TC} either in the center-of-mass or in laboratory reference frame. Similarly, the participant projectile lies in the rapidity range $[y_{P_{\min}} . y_{P_{\max}}]$, and its midrapidity is y_{PC}. The rapidity of the center-of-mass system of collisions is y_C (in the center-of-mass reference frame, $y_C = 0$). The emission points with the same rapidity, y_x, in the cylinder cut region form a cross section (emission source) in the rapidity space.

The particle emission from each source is assumed to be isotropic in the source rest frame. Let z denote the direction of the incident projectile. The three components $(p_{x,y,z})$ of par-

---

Received 1 November 2004
* Supported by NSFC (10275042, 10475054)

1) E-mail: liufh@dns.sxtu.edu.cn

ticle momentum in the source rest frame are assumed to have Gaussian distributions with the same width σ_p. Then, the transverse momentum ($p_T=\sqrt{p_x^2+p_y^2}$) has a Rayleigh distribution.

A Monte Carlo method is used in our calculation. The particles are randomly produced in the target and projectile cylinders. Let R_1, R_2, and R_3 denote the even random variables distributed in $[0,1]$, in the source rest frame, the transverse and longitudinal momenta can be given by

$$p_T=\sigma_p\sqrt{-2\ln R_1} \tag{1}$$

and

$$p_z=\sigma_p\sqrt{-2\ln R_2}\cos(2\pi R_3) \tag{2}$$

respectively. It is known that the parameter σ_p in Eqs.(1) and (2) is related to the temperature T of the emission source. Let m be the mass of produced particle, we have $\sigma_p=\sqrt{mT}$.

Because the transverse and longitudinal flows affect the emission of particles, the final state transverse and longitudinal momenta measured in the source rest frame can be written as

$$P_T^*=k_{xy}p_T, \tag{3}$$

and

$$P_z^*=k_zp_z, \tag{4}$$

where k_{xy} and k_z denote the transverse and longitudinal flow strengths, respectively. Generally speaking, $k_{xy,z}>1$ means an expansion flow, $k_{xy,z}<1$ means a contraction flow, while $k_{xy,z}=1$ means that there is no flow. The physics condition gives $k_{xy,z}>0$.

The emission angle θ^* of produced particle in the source rest frame is given by

$$\theta^*=\arctan\frac{P_T^*}{P_z^*}=\arctan\frac{k_{xy}p_T}{k_zp_z}=$$
$$\arctan\frac{k\sqrt{-\ln R_1}}{\sqrt{-\ln R_2}\cos(2\pi R_3)}, \tag{5}$$

where $k=k_{xy}/k_z$ is a free parameter which can be obtained by fitting experimental data. In the study of emission angle, we do not need to know k_{xy} and k_z. Instead, the ratio k is an important parameter in our calculation. $k>1$ means a relative strong transverse flow, $k<1$ means a relative strong longitudinal flow, while $k=1$ means an isotropic emission. In the case of $k=1$, the strengths of the transverse and longitudinal flows are the same (zero or non-zero). Considering the expression of k, we have $k_{xy}=k$ in the case of $k_z=1$.

According to the definition, the pseudorapidity variable η^* measured in the source rest frame can be given by

$$\eta^*=-\ln\tan\frac{\theta^*}{2}=$$
$$-\ln\tan\left[\frac{1}{2}\arctan\frac{k\sqrt{-\ln R_1}}{\sqrt{-\ln R_2}\cos(2\pi R_3)}\right]. \tag{6}$$

One can see that the parameter σ_p does not appear in the expression of η^*. The rapidity variable y^* in the source rest frame in terms of the pseudorapidity variable η^* can be expressed as[7]

$$y^*=\frac{1}{2}\ln\left[\frac{\sqrt{P_T^{*2}\cosh^2\eta^*+m^2}+P_T^*\sinh\eta^*}{\sqrt{P_T^{*2}\cosh^2\eta^*+m^2}-P_T^*\sinh\eta^*}\right]. \tag{7}$$

In the laboratory reference frame or the center-of-mass reference frame, the rapidity variable y is obtained by

$$y=y^*+y_x. \tag{8}$$

The pseudorapidity variable η can be obtained by [7]

$$\eta=\frac{1}{2}\ln\left[\frac{\sqrt{m_T^2\cosh^2y-m^2}+m_T\sinh y}{\sqrt{m_T^2\cosh^2y-m^2}-m_T\sinh y}\right], \tag{9}$$

where $m_T=\sqrt{P_T^{*2}+m^2}$ is the transverse mass and it is invariant in the source reference frame, the laboratory reference frame, and the center-of-mass reference frame.

The relationships among $y_{P_{\max}}$, y_{PC}, $y_{P_{\min}}$, y_C, $y_{T_{\max}}$, y_{TC}, and $y_{T_{\min}}$ are

$$y_{PC}-y_C=y_C-y_{TC}\equiv\Delta y, \tag{10}$$

and

$$y_{P_{\max}}-y_{PC}=y_{PC}-y_{P_{\min}}=$$
$$y_{T_{\max}}-y_{TC}=y_{TC}-y_{T_{\min}}\equiv\delta y, \tag{11}$$

where Δy and δy are the rapidity shifts. Generally speaking, y_C should be the rapidity of the center-of-mass system of collisions, the peak position of particle rapidity distribution, or the mean value of particle rapidities.

Fig.1(a) presents the rapidity distributions in the center-of-mass system for π^- and π^+ produced in Au-Au collisions at $1A$ GeV(SIS energy). The circles and squares are the experimental data of the FOPI Collaboration[8]. The experimental data are compared with the Monte Carlo results (points and curves with 5×10^3 and 5×10^5 particles respectively) calculated using the model code. The points and curves in Fig.1(a) represent the rapidity calculation of OCM, which are in good agreement with the FOPI experimental data. The FOPI data are minimum biased but do not include pions with transverse momentum smaller than 0.1 GeV/c. As stated in Ref.[8], this cut has considerable influence on the extracted rapidity distribution. In the calculation, the fitted values of y_C, Δy, δy, k, T, and χ^2/degrees of freedom(*dof*) are given in Table 1. One can see that two completely overlapping cylinders and a relatively strong longitudinal flow ($k < 1$) are equally good for the π^- and π^+ rapidity distributions in 1A GeV Au-Au collisions and can describe the rapidity distribution at SIS energy.

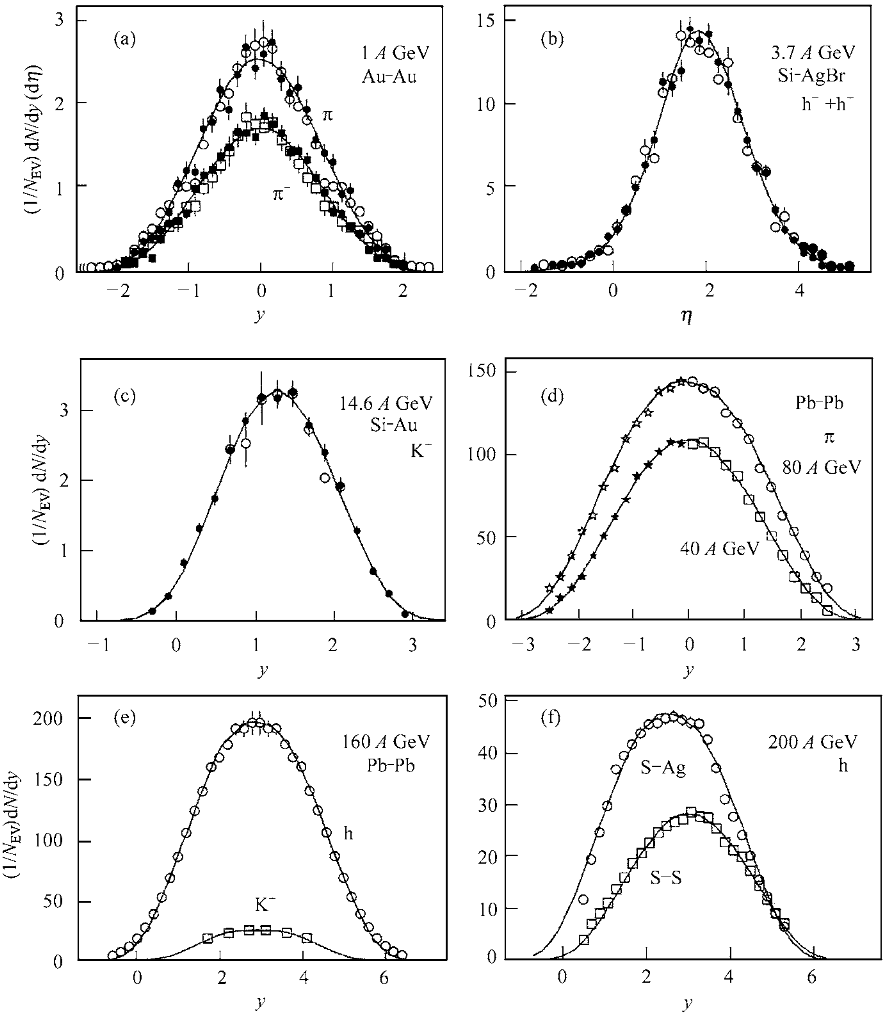

Fig.1. Rapidity (or pseudorapidity) distributions of charged-particles produced in fixed-target nucleus-nucleus collisions.
The circles and squares are the experimental data quoted in Refs.[8—18]; The points and curves are our corresponding calculations of OCM.
In Fig.1(a), the experimental data do not include pions with transverse momentum smaller than 0.1 GeV/c[8];
In Fig.1(d), the stars are reflected around midrapidity.

Fig.1(b) presents the pseudorapidity distributions in the laboratory reference frame for relativistic singly charged particles produced in central Si-AgBr collisions at 3.7A GeV (Dubna energy). The circles are the experimental data quoted from Ref.[9]. Fig.1(c) exhibits the rapidity distributions of K^+ particles produced in central Si-Au collisions at 14.6A GeV (AGS energy) in the laboratory reference frame reported by E802 Collaboration[10,11]. The experimental data shown in Figs.1(b) and 1(c) are compared with 5×10^3 and 5×10^5 particles generated for each of beams at different energies using the Monte Carlo calculation shown as points and curves in the figures. The pseudorapidity and rapidity distribution of calculated events/particles are in good agreement with the experimental data and the shapes of experimental distributions are reproduced well in each case. The fitted values of parameters y_C, Δy, δy, k, T, and χ^2/dof are tabulated in Table 1. One can observe again that OCM calculation can describe the (pseudo) rapidity distributions in most central nucleus-nucleus collisions at the Dubna and AGS energies respectively, where it is assumed that no spectator part is left from the projectile.

Table 1. Parameter values used in the calculation

figure	collision	energy	particle	y_C	Δy	δy	k	T	χ^2/dof
1(a)	Au-Au	1*A* GeV	π^-	0.00	0.00	0.72	0.71	125	0.422
1(a)	Au-Au	1*A* GeV	π^+	0.00	0.00	0.72	0.71	125	0.501
1(b)	Si-AgBr	3.7*A* GeV	$h^- + h^+$	1.41	0.00	0.75	0.71	130	0.431
1(c)	Si-Au	14.6*A* GeV	K^+	1.30	0.00	0.80	0.71	155	0.211
1(d)	Pb-Pb	40*A* GeV	π^-	0.00	0.00	1.42	0.71	162	0.156
1(d)	Pb-Pb	80*A* GeV	π^-	0.00	0.00	1.62	0.71	178	0.307
1(e)	Pb-Pb	160*A* GeV	h^-	2.91	0.00	1.76	0.71	280	0.524
1(e)	Pb-Pb	160*A* GeV	K^+	2.91	0.00	1.50	0.71	280	0.411
1(f)	S-S	200*A* GeV	h^-	3.05	0.00	1.63	0.71	288	0.669
1(f)	S-Ag	200*A* GeV	h^-	2.60	0.00	1.77	0.71	288	0.505
3(a)	Si-Ag/Br	4*T* GeV	$h^- + h^+$	-0.20	0.80	1.80	0.71	280	1.733
2(a)	Au-Au	$\sqrt{s} = 130A$ GeV	$h^- + h^+$	0.00	1.38	2.10	0.63	350	0.528
2(b)	Au-Au	$\sqrt{s} = 200A$ GeV	$h^- + h^+$	0.00	1.40	2.29	0.56	383	0.620
3(b)	Ca-C	100*A* TeV	$h^- + h^+$	-0.20	1.83	2.80	0.53	380	1.804

In order to compare our OCM calculation with the experimental data at SPS energies, we have taken various experimental rapidity distributions data reported by NA35 and NA49 collaborations respectively for different charged particles produced in central nulceus-nucleus collisions. Fig. 1(d) exhibits the rapidity distributions for π^--particles produced in central Pb-Pb collisions at 40*A* and 80*A* GeV in center-of-mass frame reported by NA49 Collaboration[12] and the stars are reflected around midrapidity. The rapidity distributions in the laboratory reference frame for negatively charged hadrons (h^--) and K^+-particles produced in central Pb-Pb collisions at 160*A* GeV reported by NA49 Collaboration[13—15] are also shown in Fig. 1(e). In Fig. 1(f), the rapidity distributions of h^--particles produced in central S-S and S-Ag collisions at 200*A* GeV in lab frame of reference are shown. The circles and squares shown in Figs. 1(d) – 1(f) are the experimental data of the NA49 and NA35 Collaborations[12—18] along with the corresponding calculations from OCM model shown as curves in the figures. In general, one can notice that the model reproduces the rapidity distribution of different charged-particles quite well and the best results at SPS energy are obtained. The values of y_C, Δy, δy, k, T, and χ^2/dof are given in Table 1.

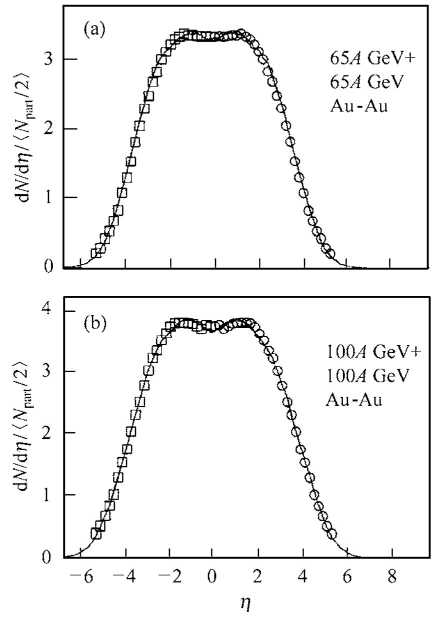

Fig.2. Pseudorapidity distributions of charged particles produced in ntral Au-Au collisions at $\sqrt{s} = 130A$ GeV(a) and 200*A* GeV(b). The circles are the experimental data of the PHOBOS Collaboration[19] and the squares are reflected around $\eta = 0$. The curves are our corresponding calculations of OCM.

Recently, the pseudorapidity distributions of charged particles produced in central Au-Au collisions at center-of-mass energy $\sqrt{s} = 130A$ and $200A$ GeV (RHIC energies) have been reported by the PHOBOS Collaboration[19] and are shown in Figs. 2(a) and 2(b) by circles. The squares in the figures are reflected around midrapidity. The same distributions obtained from OCM calculation based on 5×10^6 particles are shown in the figures (solid curves) and are consistent with the RHIC data. The fitted values of y_C, Δy, δy, k, T, and χ^2/dof are given in Table 1. One can observe that two partly overlapping cylinders and a relative strong longitudinal flow ($k < 1$) can describe the charged particle pseudorapidity distributions at the RHIC energies.

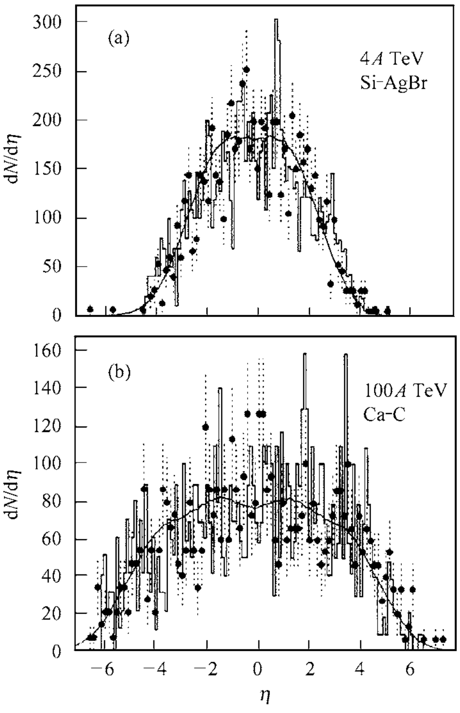

Fig. 3. Pseudorapidity distribution of charged particles produced in a 4*A* TeV central Si-Ag/Br collision (a) and a 100*A* TeV central Ca-C collision observed in a cosmic ray experiment. The histograms are the experimental data of the JACEE Collaboration[20]; The points and curves are our corresponding calculations of OCM.

Fig. 3 shows the pseudorapidity distributions in the center-of-mass system for charged particles produced in a 4*A* TeV central Si-Ag/Br collision (a) and a 100*A* TeV central Ca-C collision (b) observed in a cosmic ray experiment. The histograms shown in Fig. 3 are the experimental data of the JACEE Collaboration[20]. The points and curves are our Monte Carlo calculated results with N and 5×10^6 particles respectively, where N denotes the normalization constant. The values of y_C, Δy, δy, k, T, and χ^2/dof are given in Table 1. One can see that two partly overlapping cylinders and a relative strong longitudinal flow ($k < 1$) give qualitatively a description of the mean trend (curves) and the fluctuation (points) of charged particle pseudorapidity distributions in the two JACEE events.

The RHIC energies ($\sqrt{s} = 130A$ and $200A$ GeV (Fig. 3)) are in between 4*A* TeV (Fig. 2(a)) and 100*A* TeV (Fig. 2(b)) (the energies of two individual JACEE events[11]). Differing from other figures, Fig. 3 is for two single events. For Fig. 3, the value of rapidity $y_C = -0.20$ was taken in our model calculation while this value should be zero for pseudorapidity distributions investigated in the centre-of-mass system. The non-zero y_C can be regarded as a systematic deviation.

From Figs. 1—3 and Table 1 one can see that two overlapping cylinders and a relatively strong longitudinal flow give a description of the experimental data over an energy range from 1*A* GeV to 100*A* TeV. In a wide energy range, from 1*A* GeV to 200*A* GeV, the relative strengths of the longitudinal flows are the same and the target and projectile cylinders overlap completely. From 4*A* TeV to 100*A* TeV, the two cylinders overlap partly. The temperature of the interacting system increases with increasing the incident energy. For Pb-Pb collisions at 160*A* GeV, the temperature is greater than 200 MeV. A higher temperature is obtained at the RHIC energies.

In the model, the free parameter k denotes the flow. $k > 1$ means a relatively strong transverse flow, $k < 1$ means a relatively strong longitudinal flow, while $k = 1$ means the same strong transverse and longitudinal flows or means that there are no transverse or longitudinal flows. A Monte Carlo calculation gives a description of the experimental (pseudo) rapidity fluctuations. The calculated results of the overlapping cylinder model with flows are in agreement with the experimental data over an energy range from 1*A* GeV to 100*A* TeV.

References

1 Werner K. Phys. Rep., 1993, **232**: 87—299

2 Westfall G D, Gosset J, Johansen O J et al. Phys. Rev. Lett., 1976, **37**: 1202—1205

3 LIU Fu-Hu, Panebratsev Y A. Nucl. Phys., 1998, **A641**: 379—385

4 LIU Fu-Hu. Phys. Rev., 2002, **C66**: 047902-1—047902-3

5 LIU Fu-Hu, ZHANG Dong-Hai, DUAN Mai-Ying. Euro. Phys. Lett., 2003, **61**: 736—741

6 LIU Fu-Hu. Phys. Lett., 2004, **B583**: 68—72

7 WONG C Y. *Introduction to High-Energy Heavy-Ion Collisions*. Singapore: World Scientific, 1994. 24—25

8 Pelte D, Hafele E, Best D et al (FOPI Collaboration). Z. Phys., 1997, **A357**: 215—234

9 Singh B K, Tuli S K. Nucl. Phys., 1996, **A602**: 487—501

10 Abbott T, Akiba Y, Beavis D et al (E802 Collaboration). Phys. Rev., 1993, **C47**: 1351—1355

11 Abbott T, Akiba Y, Beavis D et al (E802 Collaboration). Phys. Rev., 1994, **C50**: 1024—1047

12 van Leeuwen M (NA49 Collaboration). nucl-ex/0208014

13 Appelshäuser H, Bachler S, Bailey S J et al (NA49 Collaboration). Phys. Rev. Lett., 1999, **82**: 2471—2475

14 Toy M Y. Ph. D Thesis, University of California, Los Angeles, USA, 1999

15 Bormann C, Alber T, Appelshäuser H et al (NA49 Collaboration). J. Phys., 1997, **G23**: 1817—1825

16 Stroebele H, Bamberger A, Bangert D et al (NA35 Collaboration). Z. Phys., 1988, **C38**: 89—93

17 Rohrich D, Alber T, Bachler J et al (NA35 Collaboration). Nucl. Phys., 1994, **A566**: 35c—44c

18 Rohrich D. Hot and Dense Nuclear Matter, In: Greiner W, Socker H, Gallmann Aed. NATO ASI Physics, **B335**. New York: Plenum Press, 1994. 505

19 Nouicer R (PHOBOS Collaboration). nucl-ex/0208003

20 Burnett T H, Dake S, Fuki M et al (JACEE Collaboration). Phys. Rev. Lett., 1983, **50**: 2062—2065

高能核-核碰撞中粒子的(赝)快度分布与重叠柱模型*

宋福 刘福虎1)

(山西师范大学现代物理研究所 临汾 041004)

摘要 应用重叠柱模型描述了高能核-核碰撞中带电粒子的快度(或赝快度)分布.对目前加速器上的固定靶实验而言,观察到了相同相对强度的纵向流,两个完全重叠的热化柱能够描述实验数据.在更高能量范围(4A TeV以上),观察到了更强的纵向流,这时需要两个部分重叠的热化柱来描述实验数据.用重叠柱模型计算得到的(赝)快度分布与1A GeV到100A TeV能区的实验结果符合.

关键词 核-核碰撞 (赝)快度分布 重叠柱模型

2004-11-01 收稿

* 国家自然科学基金(10275042,10475054)资助

1) E-mail: liufh@dns.sxtu.edu.cn